

UC Santa Barbara

UC Santa Barbara Previously Published Works

Title

Nitrogen-passivated dielectric/InGaAs interfaces with sub-nm equivalent oxide thickness and low interface trap densities

Permalink

<https://escholarship.org/uc/item/2fs9c0fs>

Journal

Applied Physics Letters, 102(2)

Authors

Chobpattana, Varistha
Son, Junwoo
Law, Jeremy
et al.

Publication Date

2013-01-15

Peer reviewed

Nitrogen-passivated dielectric/InGaAs interfaces with sub-nm equivalent oxide thickness and low interface trap densities

Varistha Chobpattana,¹ Junwoo Son,¹ Jeremy J. M. Law,¹ Roman Engel-Herbert,² Cheng-Ying Huang,³ and Susanne Stemmer^{1,a)}

¹Materials Department, University of California, Santa Barbara, California 93106-5050, USA

²Department of Materials Science and Engineering, Pennsylvania State University, University Park, Pennsylvania 16802, USA

³Department of Electrical and Computer Engineering, University of California, Santa Barbara, California 93106, USA

(Received 14 November 2012; accepted 26 December 2012; published online 15 January 2013)

We report on the electrical characteristics of HfO₂ and HfO₂/Al₂O₃ gate dielectrics deposited on *n*-In_{0.53}Ga_{0.47}As by atomic layer deposition, after *in-situ* hydrogen or nitrogen plasma surface cleaning procedures, respectively. It is shown that alternating cycles of nitrogen plasma and trimethylaluminum prior to growth allow for highly scaled dielectrics with equivalent oxide thicknesses down to 0.6 nm and interface trap densities that are below $2.5 \times 10^{12} \text{ cm}^{-2} \text{ eV}^{-1}$ near midgap. It is shown that the benefits of the nitrogen plasma surface cleaning procedure are independent of the specific dielectric. © 2013 American Institute of Physics. [<http://dx.doi.org/10.1063/1.4776656>]

A major obstacle facing the development of metal-oxide-semiconductor field effect transistors with In_{0.53}Ga_{0.47}As channels is the high density of traps (D_{it}) at the gate dielectric/III-V semiconductor interface. Typical capacitance-voltage (CV) curves of unpinned metal-oxide-semiconductor capacitors (MOSCAPs) on *n*-In_{0.53}Ga_{0.47}As show a frequency-dependent “hump” at negative biases, characteristic of midgap D_{it} response.^{1,2} Most studies have focused on Al₂O₃ or HfO₂/Al₂O₃ bilayers, as Al₂O₃ is believed to allow for lower D_{it} than HfO₂,³ although deposition methods other than atomic layer deposition (ALD) have shown promising results for HfO₂.⁴ The low dielectric constant of Al₂O₃ limits scaling of the equivalent oxide thickness (EOT). To reduce the D_{it} , various passivation approaches have been examined in the literature, including treatment with sulfur containing agents,^{5,6} As-decapping,^{7,8} hydrogen plasma,^{9,10} and hydrogenation/nitridization.^{11,12} These approaches have been relatively successful in reducing the midgap D_{it} , lowering the “hump” at negative biases in CV, and producing steep movement in frequency of normalized conductance maxima with gate bias. The EOTs of such well-behaved gate stacks have, however, not yet been aggressively scaled, and accumulation capacitance densities on *n*-In_{0.53}Ga_{0.47}As are typically below $2 \mu\text{F}/\text{cm}^2$ (at 1 MHz).^{4,9,13–16} Conversely, more scaled dielectrics exhibit a very large frequency-dependent “hump” at negative biases,^{17,18} characteristic of a large midgap D_{it} , or are pinned before the band bending reaches midgap, as evidenced by failure to reach the depletion capacitance density as determined by the doping level. In this letter, we show that *in-situ* surface cleaning involving alternating cycles of nitrogen plasma and trimethylaluminum (TMA) pulses prior to ALD of different dielectrics allows for significantly reduced midgap D_{it} and simultaneous scaling of the EOT to well below 1 nm.

Substrates were 300-nm-thick, *n*-type In_{0.53}Ga_{0.47}As (Si: $1.5\text{--}3 \times 10^{17} \text{ cm}^{-3}$) grown by molecular beam epitaxy on (001) *n*⁺-InP (Si: $3 \times 10^{18} \text{ cm}^{-3}$), cleaned in 10:1 deionized

H₂O:HCl for 2 min or buffered HF for 3 min, respectively. Samples were transferred to the ALD reactor (Oxford Instruments FlexAL ALD) within a few minutes, and exposed to either alternating hydrogen/TMA or nitrogen plasma/TMA pulses. Each cycle consisted of a hydrogen or nitrogen plasma pulse (20 mTorr H₂ or N₂, inductively coupled plasma power of 100 W for 2 s), followed by TMA (40 ms), a second hydrogen or nitrogen plasma pulse, followed by 2 s of Ar purge and 10 s of a H₂ or N₂ stabilization step. The benefits of alternating TMA/hydrogen plasma cycles, rather than using only hydrogen plasma, have been discussed elsewhere.⁹ The substrate temperature was 300 °C. The chamber reactor was at 200 mTorr. The two different surface treatments will be referred to hereafter as hydrogen and nitrogen plasma samples, respectively. A separate study (not shown here) showed that the optimum number of cycles was 5 and 10 for hydrogen plasma and nitrogen plasma, respectively. The larger number of cycles needed for nitrogen plasma cleaning is consistent with reports that hydrogen radicals are more effective in removing surface layers than nitrogen radicals.¹⁹ Increasing the number of cycles beyond the optimum number resulted in a high midgap D_{it} , most likely due to damage to the semiconductor.²⁰ Al₂O₃ was deposited using 500 ms of TMA followed by 7 s of Ar gas purge and 500 ms of deionized water followed by 7 s of Ar purge. The reactor was pumped for 7 s, followed by an Ar purge at 200 mTorr for 5 s. TEMAH (tetrakis[ethylmethylamino]hafnium) was used to deposit HfO₂. Before HfO₂ deposition for HfO₂/Al₂O₃ bilayers (Al₂O₃ being the first layer, interfacing with the In_{0.53}Ga_{0.47}As) the sample was moved to the load lock, while the reactor was conditioned with 20 cycles of HfO₂. The growth rates for all dielectrics were $\sim 1.1 \text{ \AA}/\text{cycle}$. After dielectric deposition, samples were annealed in a tube furnace at 400 °C for 15 min in forming gas (95% of N₂ and 5% of H₂). For MOSCAPs, 80-nm-thick Ni gate electrodes were deposited through a shadow mask by thermal evaporation. CV and conductance-voltage measurements were performed at room temperature and frequencies between 1 kHz and 1 MHz

^{a)}Electronic mail: stemmer@mrl.ucsb.edu.

in the dark. The Terman and conductance methods were used to estimate the D_{it} and its distribution in the band gap, as described elsewhere.^{1,21,22}

Figure 1 shows the CV data, conductance maps, and D_{it} distribution, extracted by the Terman method, for MOSCAPs with 3.3-nm-HfO₂/1.1-nm-Al₂O₃ bilayer dielectrics. The data shown in Fig. 1 are from samples subjected to hydrogen plasma (left column) or nitrogen plasma (right column), respectively. Both samples have comparable accumulation capacitance densities of $\sim 2.1 \mu\text{F}/\text{cm}^2$ at 1 MHz, corresponding to an EOT of ~ 0.7 nm. The frequency dispersion at negative biases in CV is significantly smaller for the nitrogen plasma sample, indicating a lower midgap D_{it} .^{1,2} The nitrogen-plasma MOSCAP also shows a reduced frequency dispersion in accumulation, which may be related to a lower midgap D_{it} .²³ We note that highly scaled gate stacks typically show large frequency dispersion in accumulation, and possible reasons are discussed elsewhere.^{23,24} An estimate for the D_{it} near midgap can be obtained from room-temperature conductance maps,²² shown in Figs. 1(c) and 1(d), which also indicate how efficient

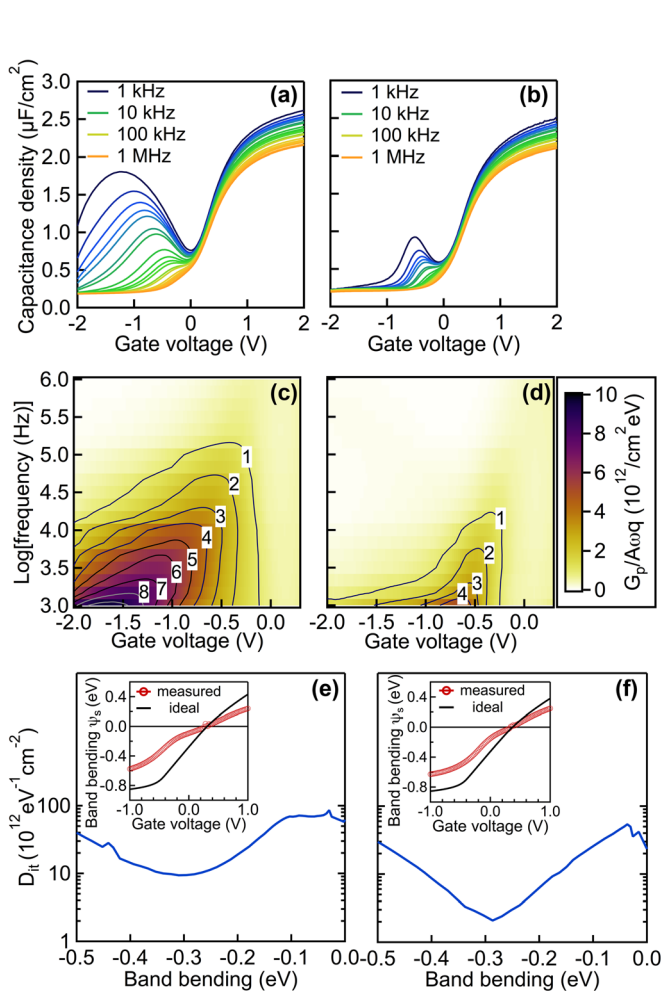


FIG. 1. In_{0.53}Ga_{0.47}As MOSCAPs with HfO₂/Al₂O₃ bilayers. (a) and (b) CV characteristics as a function of frequency; (c) and (d) Normalized parallel conductance map, showing $(G_p/A\omega q)_{\max}$ as a function of gate voltage and frequency; (e) and (f) D_{it} distribution extracted using the Terman method. The insets in (e) and (f) show the extracted band bending as a function of gate voltage. The data shown in the left column, (a), (c), and (e), are from a sample subjected to pre-deposition surface treatment with cycles of hydrogen plasma and TMA. The data shown in the right column, (b), (d), and (f), are from a sample subjected to pre-deposition surface treatment with cycles of nitrogen plasma and TMA.

the Fermi-level moves as a function of gate bias.²⁵ The conductance maps show the normalized conductance peaks, $(G_p/A\omega q)_{\max}$, where G_p is the parallel conductance, A is the capacitor area, ω is the frequency, and q is the elemental charge. The $(G_p/A\omega q)_{\max}$ values are proportional to D_{it} (by approximately a factor of 2.5).²⁶ They shift more than two orders of magnitude in frequency as the gate bias is changed between 0 and -1 V, which indicates efficient movement of the Fermi-level around midgap in both samples. The lower normalized parallel conductance peak values for the nitrogen plasma sample [Fig. 1(d)], and its narrower trace, suggests a lower D_{it} and larger band bending in response to a change in gate bias.

The D_{it} distribution over a wider range of the band gap was quantified by the Terman method,²¹ and the results are shown in Figs. 1(e) and 1(f) as a function of band bending. We note that the Terman method provides a more conservative estimate of the D_{it} near the band edges than the temperature-dependent conductance studies, for reasons that

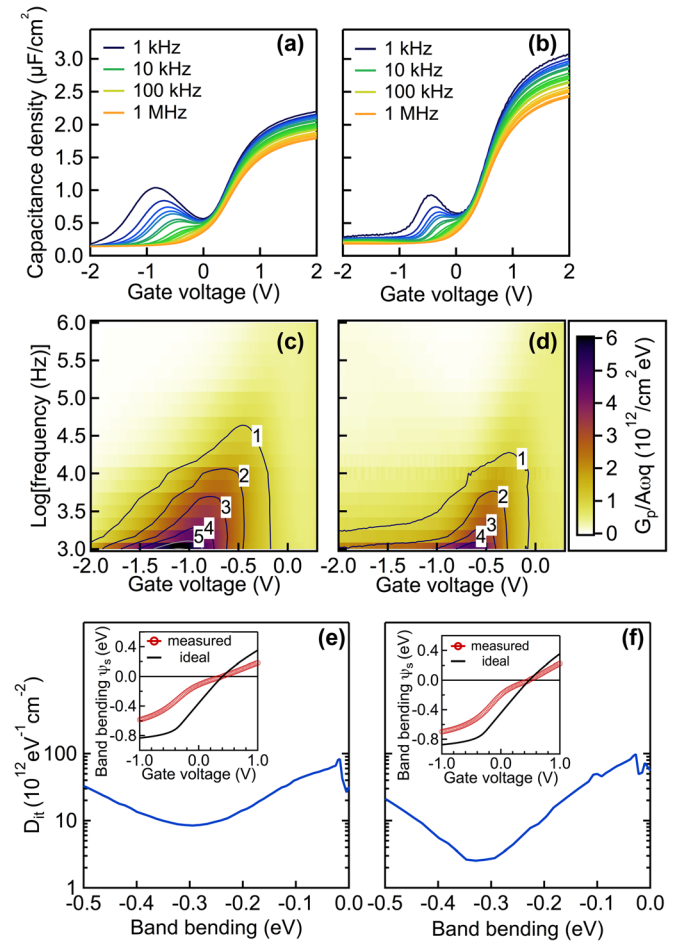


FIG. 2. In_{0.55}Ga_{0.47}As MOSCAPs with HfO₂ dielectrics. (a) and (b) CV characteristics as a function of frequency; (c) and (d) normalized parallel conductance map, showing $(G_p/A\omega q)_{\max}$ as a function of gate voltage and frequency; (e) and (f) D_{it} distribution extracted using the Terman method. The insets in (e) and (f) show the extracted band bending as a function of gate voltage. The data shown in the left column, (a), (c), and (e), are from a sample subjected to pre-deposition surface treatment with cycles of hydrogen plasma and TMA. The data shown in the right column, (b), (d), and (f), are from a sample subjected to pre-deposition surface treatment with cycles of nitrogen plasma and TMA. The two HfO₂ films have different physical thicknesses (5.5 nm and 4.4. nm, respectively, for hydrogen and nitrogen plasma samples).

are still under debate, but that may include a larger contribution of slow traps to the D_{it} extracted from the Terman method.¹ The insets in Figs. 1(e) and 1(f) compare the ideal band bending with the experimental band bending. For both samples, the band bending exceeds half of the $\text{In}_{0.53}\text{Ga}_{0.47}\text{As}$ band gap. The midgap D_{it} is, however, significantly different in the two samples. The minimum D_{it} for the hydrogen plasma sample is just below $1 \times 10^{13} \text{ cm}^{-2} \text{ eV}^{-1}$ at approximately 0.3 eV below the conduction band, whereas for the nitrogen plasma sample, it is $2 \times 10^{12} \text{ cm}^{-2} \text{ eV}^{-1}$, which is almost an order of magnitude smaller. The nitrogen plasma clean also results in reduced leakage.²⁷

The effect of nitrogen plasma cleaning on $\text{HfO}_2/\text{In}_{0.53}\text{Ga}_{0.47}\text{As}$ interfaces is shown in Fig. 2. A HfO_2 MOSCAP with an EOT of $\sim 1 \text{ nm}$ (5.5 nm physical thickness) cleaned using the hydrogen plasma sequence is shown in the left column of Fig. 2, and a HfO_2 MOSCAP with an EOT of $\sim 0.6 \text{ nm}$ (maximum accumulation capacitance density of $2.4 \mu\text{F}/\text{cm}^2$ at 1 MHz, 4.4 nm physical thickness) cleaned using the nitrogen plasma sequence is shown in the right column. Attempts to further reduce the thickness of the HfO_2 for the hydrogen plasma cleaned MOSCAPs resulted in unacceptably large midgap D_{it} . This is likely caused by poor wetting, which results in air-exposed $\text{In}_{0.53}\text{Ga}_{0.47}\text{As}$ surfaces that have high D_{it} . Atomic force microscopy images showed that films on hydrogen plasma cleaned surfaces were rougher, consistent with poorer wetting.²⁷ The HfO_2 on the nitrogen plasma cleaned surface shows higher frequency dispersion in accumulation because of its lower thickness.²³ Both conductance maps, shown in Figs. 2(c) and 2(d), and the D_{it} distribution determined by the Terman method, shown in Figs. 2(e) and 2(f), indicate a significantly reduced midgap D_{it} and large band bending with applied voltage for the nitrogen plasma sample, despite its very low EOT. The minimum D_{it} is about $2.5 \times 10^{12} \text{ cm}^{-2} \text{ eV}^{-1}$, which is only slightly higher than that of the $\text{HfO}_2/\text{Al}_2\text{O}_3$ bilayer sample, which also had a slightly higher EOT. We note that in all cases the type of cleaning procedure used had relatively little influence on the D_{it} near the conduction band edge.

In summary, we have shown that pre-deposition *in-situ* cleaning using alternating cycles of remote nitrogen plasma and TMA allows for scaling of both $\text{HfO}_2/\text{Al}_2\text{O}_3$ bilayers and HfO_2 gate stacks to EOTs approaching 0.5 nm, while maintaining a midgap D_{it} in the low $10^{12} \text{ cm}^{-2} \text{ eV}^{-1}$ range. Further studies are needed to determine the mechanism(s) by which activated nitrogen acts as a passivation agent, but it is clear from this study that nitrogen is more beneficial than hydrogen radicals. As with other treatments that resulted in improved electrical characteristics of dielectric/ $\text{In}_{0.53}\text{Ga}_{0.47}\text{As}$ interfaces,^{28,29} the improvements are largely with the midgap D_{it} , which appears to be determined by defects in the semiconductor, independent of the specific dielectric. The results also show that interfaces with Al_2O_3 are not fundamentally superior in terms of achieving low D_{it} than HfO_2 , and thus scaling of high-k/III-V interfaces to sub-0.5 nm EOT by further reducing the HfO_2 thickness or using dielectrics with even higher permittivities than HfO_2 should be feasible.

V.C. thanks Adam Kajdos for help with the AFM images. The authors gratefully acknowledge support for this work by

the Semiconductor Research Corporation through the Non-classical CMOS Research Center (Task ID 1437.008). J.S. was supported by NSF (award number ECCS-1125017). A portion of this work was performed in UCSB's nanofabrication facility, which is part of the NSF-funded NNIN network.

- ¹R. Engel-Herbert, Y. Hwang, and S. Stemmer, *J. Appl. Phys.* **108**, 124101 (2010).
- ²I. Krylov, L. Kornblum, A. Gavrilov, D. Ritter, and M. Eizenberg, *Appl. Phys. Lett.* **100**, 173508 (2012).
- ³R. Suzuki, N. Taoka, M. Yokoyama, S. Lee, S. H. Kim, T. Hoshii, T. Yasuda, W. Jevasuwan, T. Maeda, O. Ichikawa *et al.*, *Appl. Phys. Lett.* **100**, 132906 (2012).
- ⁴Y. Hwang, V. Chobpattana, J. Y. Zhang, J. M. LeBeau, R. Engel-Herbert, and S. Stemmer, *Appl. Phys. Lett.* **98**, 142901 (2011).
- ⁵B. J. Skromme, C. J. Sandroff, E. Yablonovitch, and T. Gmitter, *Appl. Phys. Lett.* **51**, 2022 (1987).
- ⁶E. O'Connor, B. Brennan, V. Djara, K. Cherkaoui, S. Monaghan, S. B. Newcomb, R. Contreras, M. Mijovic, G. Hughes, M. E. Pemble *et al.*, *J. Appl. Phys.* **109**, 024101 (2011).
- ⁷E. J. Kim, E. Chagarov, J. Cagnon, Y. Yuan, A. C. Kummel, P. M. Asbeck, S. Stemmer, K. C. Saraswat, and P. C. McIntyre, *J. Appl. Phys.* **106**, 124508 (2009).
- ⁸Y. Hwang, R. Engel-Herbert, and S. Stemmer, *Appl. Phys. Lett.* **98**, 052911 (2011).
- ⁹A. D. Carter, W. J. Mitchell, B. J. Thibeault, J. J. M. Law, and M. J. W. Rodwell, *Appl. Phys. Express* **4**, 091102 (2011).
- ¹⁰W. Melitz, J. Shen, T. Kent, A. C. Kummel, and R. Droopad, *J. Appl. Phys.* **110**, 013713 (2011).
- ¹¹F. Capasso and G. F. Williams, *J. Electrochem. Soc.* **129**, 821 (1982).
- ¹²A. Callegari, P. D. Hoh, D. A. Buchanan, and D. Lacey, *Appl. Phys. Lett.* **54**, 332 (1989).
- ¹³M. Radosavljevic, G. Dewey, J. M. Fastenau, J. Kavalieros, R. Kotlyar, B. Chu-Kung, W. K. Liu, D. Lubyshev, M. Metz, K. Millard *et al.* in *IEEE International Electron Devices Meeting (IEDM)* (2010), p. 6.1.1.
- ¹⁴I. Krylov, A. Gavrilov, D. Ritter, and M. Eizenberg, *Appl. Phys. Lett.* **99**, 203504 (2011).
- ¹⁵E. J. Kim, L. Q. Wang, P. M. Asbeck, K. C. Saraswat, and P. C. McIntyre, *Appl. Phys. Lett.* **96**, 012906 (2010).
- ¹⁶R. Suzuki, N. Taoka, M. Yokoyama, S.-H. Kim, T. Hoshii, T. Maeda, T. Yasuda, O. Ichikawa, N. Fukuhara, M. Hata *et al.*, *J. Appl. Phys.* **112**, 084103 (2012).
- ¹⁷S. Koveshnikov, N. Goel, P. Majhi, H. Wen, M. B. Santos, S. Oktyabrsky, V. Tokranov, R. Kambhampati, R. Moore, F. Zhu *et al.*, *Appl. Phys. Lett.* **92**, 222904 (2008).
- ¹⁸T. D. Lin, Y. H. Chang, C. A. Lin, M. L. Huang, W. C. Lee, J. Kwo, and M. Hong, *Appl. Phys. Lett.* **100**, 172110 (2012).
- ¹⁹J. Y. Yun, S. W. Rhee, S. Park, and J. G. Lee, *J. Vac. Sci. Technol. A* **18**, 2822 (2000).
- ²⁰V. Chobpattana, J. Son, and S. Stemmer (unpublished).
- ²¹R. Engel-Herbert, Y. Hwang, and S. Stemmer, *Appl. Phys. Lett.* **97**, 062905 (2010).
- ²²K. Martens, C. O. Chui, G. Brammertz, B. De Jaeger, D. Kuzum, M. Meuris, M. M. Heyns, T. Krishnamohan, K. Saraswat, H. E. Maes *et al.*, *IEEE Trans. Electron Devices* **55**, 547 (2008).
- ²³S. Stemmer, V. Chobpattana, and S. Rajan, *Appl. Phys. Lett.* **100**, 233510 (2012).
- ²⁴A. Ali, H. Madan, S. Koveshnikov, S. Oktyabrsky, R. Kambhampati, T. Heeg, D. Schlom, and S. Datta, *IEEE Trans. Electron Devices* **57**, 742 (2010).
- ²⁵H. C. Lin, G. Brammertz, K. Martens, G. de Valicourt, L. Negre, W. E. Wang, W. Tsai, M. Meuris, and M. Heyns, *Appl. Phys. Lett.* **94**, 153508 (2009).
- ²⁶E. H. Nicollian and J. R. Brews, *MOS (Metal Oxide Semiconductor) Physics and Technology* (Wiley, New York, 1982).
- ²⁷See supplementary material at <http://dx.doi.org/10.1063/1.4776656> for AFM images of HfO_2 surfaces and leakage data.
- ²⁸G. J. Burek, Y. Hwang, A. D. Carter, V. Chobpattana, J. J. M. Law, W. J. Mitchell, B. Thibeault, S. Stemmer, and M. J. W. Rodwell, *J. Vac. Sci. Technol. B* **29**, 040603 (2011).
- ²⁹Y. Hwang, R. Engel-Herbert, N. G. Rudawski, and S. Stemmer, *J. Appl. Phys.* **108**, 034111 (2010).